

Synergistic Inhibition of SARS-CoV-2 Replication Using Disulfiram/
Ebselen and RemdesivirTing Chen, Cheng-Yin Fei, Yi-Ping Chen, Karen Sargsyan, Chun-Ping Chang, Hanna S. Yuan,*
and Carmay Lim*Cite This: *ACS Pharmacol. Transl. Sci.* 2021, 4, 898–907

Read Online

ACCESS |



Metrics & More



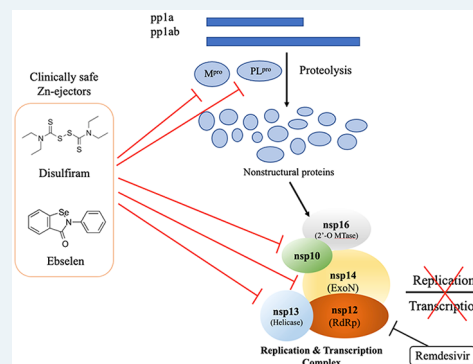
Article Recommendations



Supporting Information

ABSTRACT: The SARS-CoV-2 replication and transcription complex (RTC) comprising nonstructural protein (nsp) 2–16 plays crucial roles in viral replication, reducing the efficacy of broad-spectrum nucleoside analog drugs such as remdesivir and evading innate immune responses. Most studies target a specific viral component of the RTC such as the main protease or the RNA-dependent RNA polymerase. In contrast, our strategy is to target *multiple* conserved domains of the RTC to prevent SARS-CoV-2 genome replication and to create a high barrier to viral resistance and/or evasion of antiviral drugs. We show that the clinically safe Zn-ejector drugs disulfiram and ebselen can target conserved Zn²⁺ sites in SARS-CoV-2 nsp13 and nsp14 and inhibit nsp13 ATPase and nsp14 exoribonuclease activities. As the SARS-CoV-2 nsp14 domain targeted by disulfiram/ebselen is involved in RNA fidelity control, our strategy allows coupling of the Zn-ejector drug with a broad-spectrum nucleoside analog that would otherwise be excised by the nsp14 proofreading domain. As proof-of-concept, we show that disulfiram/ebselen, when combined with remdesivir, can synergistically inhibit SARS-CoV-2 replication in Vero E6 cells. We present a mechanism of action and the advantages of our multitargeting strategy, which can be applied to any type of coronavirus with conserved Zn²⁺ sites.

KEYWORDS: COVID-19, structural Zn sites, nsp13, nsp14, replication and transcription complex



The COVID-19 pandemic, caused by severe acute respiratory syndrome coronavirus 2 (SARS-CoV-2), is affecting billions of people around the world. The recent approval of several vaccines against SARS-CoV-2¹ would help to reduce transmission. However, it is not known how long immunity stays and whether the vaccinated person, though protected from COVID-19, may still carry the SARS-CoV-2 for some period and possibly infect others. To treat hospitalized COVID-19 patients, antivirals such as small-molecule drugs and neutralizing antibodies targeting SARS-CoV-2 are needed. Neutralizing antibodies derived from convalescent plasma obtained from a COVID-19 patient have shown only moderate success in clinical studies.² *De novo* antiviral development is lengthy and costly. A shortcut approach is to repurpose widely available, inexpensive drugs that can be easily administered against SARS-CoV-2. Most studies target a single SARS-CoV-2 protein³ such as the spike protein that mediates cell entry,⁴ the main protease (M^{pro})^{5,6} or the papain-like protease (PL^{pro})⁷ that cleaves the viral polyprotein into its constituent proteins, or the RNA-dependent RNA polymerase (RdRp) that catalyzes viral RNA synthesis.^{8,9} However, the virus may evade antiviral drugs that target a single viral protein by mutations¹⁰ or deletions,¹¹ and the spike receptor-binding domain is the most variable.¹² One strategy is to create a high

barrier to viral resistance/evasion of antiviral drugs by targeting sites with slow mutation rates in the *multiprotein* SARS-CoV-2 replication and transcription complex (RTC) that enables viral replication and transcription (see below). Here, we show that FDA-approved drugs (disulfiram/ebselen and remdesivir) can *synergistically* inhibit SARS-CoV-2 replication by targeting *conserved* sites in *multiple* nonstructural proteins (nsps) constituting the core of the RTC.

SARS-CoV-2 is an enveloped β -coronavirus containing a positive-sense single-stranded RNA (+ssRNA) genome that encodes 16 nonstructural, 4 structural, and 9 accessory proteins.¹³ It infiltrates cells by binding to human cell surface receptors such as angiotensin-converting enzyme 2 (ACE2) and possibly other cell receptors such as CD147¹⁴ via its spike glycoprotein, which upon cleavage by human proteases enables virus–cell membrane fusion (Figure 1A).^{3,15,16} Once inside, the viral RNA genome is released into the cytoplasm. Its 5' end

Received: January 15, 2021

Published: March 26, 2021



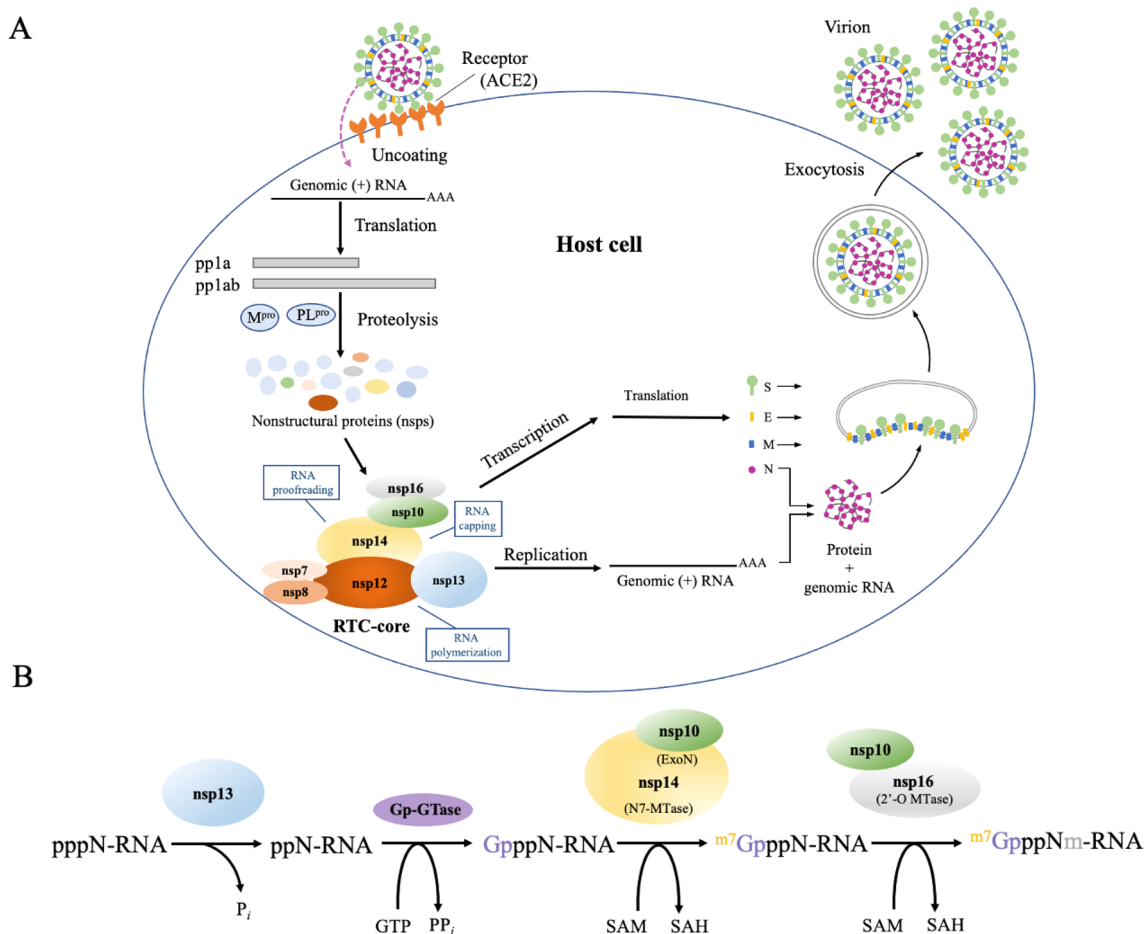


Figure 1. Importance of RTC in the SARS-CoV-2 life cycle. (A) SARS-CoV-2 enters cells by the binding of its surface spike (S) protein to human ACE2 and possibly other cell receptors. Once inside the cell, the 5' end of its genomic RNA is translated by host ribosomes to yield viral nsps. Nsp7–8, nsp10, nsp12–14, and nsp16 form the core of the viral RTC, which drives the synthesis of full-length and subsets of the genomic ssRNA. (B) Capping of newly synthesized viral mRNA is initiated by nsp13 catalyzing the hydrolysis of the 5'- γ -phosphate of the nascent pppN-RNA to ppN-RNA. A yet to be identified GTase transfers a GMP (Gp) to ppN-RNA, yielding GpppN-RNA. Subsequently, the nsp14 N7-MTase methylates the guanosine N7, forming m^7 GpppN-RNA via the demethylating coenzyme S-adenosyl methionine (SAM) to S-adenosyl homocysteine (SAH). Finally, the nsp16 2'-O-MTase demethylates SAM to SAH and adds the methyl group to the ribose 2'-O, yielding m^7 GpppNm-RNA. nsp10 is needed to activate the enzymatic activities of nsp14 N7-MTase and nsp16 2'-O-MTase.

is translated by the host protein synthesis machinery to polyproteins (pp1a and pp1ab) that are cleaved by virus-encoded proteases (M^{pro} and PL^{pro}) to 16 constituent nsps.¹⁷ The viral RTC is formed from nsp2–16¹⁸ and plays two crucial functions: (i) transcription of subsets of the viral genome to produce mRNAs that are translated into accessory and structural proteins and (ii) replication of the full-length +ssRNA genome. The viral proteins are then assembled into a virion consisting of the spike (S), envelope (E), membrane (M), and nucleocapsid (N) proteins, with the latter encapsidating the +ssRNA.¹⁸ Multiple virions leave from a single infected cell.

SARS-CoV-2 replication involves RNA synthesis, proofreading, and modification/capping. Viral RNA synthesis is catalyzed by the C-terminal RdRp domain of nsp12 with the help of nsp7 and nsp8 cofactors.^{8,19,20} RNA proofreading, the maintenance of the SARS-CoV-2 genome integrity, is carried out by the N-terminal 3'–5' exoribonuclease (ExoN) domain of nsp14, which recognizes erroneous nucleotides and catalyzes their excision.²¹ The nsp14 ExoN is stabilized by the nsp10 zinc-finger protein, which enhances its nucleolytic activity.²² Viral RNA capping, the addition of a cap structure to the newly

synthesized viral mRNAs, ensures their efficient translation by host cell ribosomes and evasion of the host immune response. Without the cap structure, the viral RNA molecules are degraded and may be detected as “non-self” by the host, triggering innate immune responses.¹⁷ SARS-CoV-2 mRNA cap synthesis involves nsp10 and four enzymes, viz., (i) nsp13 helicasetriphosphatase, (ii) an unknown guanylyltransferase (GTase), (iii) nsp14 C-terminal (N7) guanine (N7-MTase), and (iv) nsp16 2'-O-methyltransferase (2'-O-MTase). nsp10 serves as an allosteric activator of the two methyltransferase enzymes and stabilizes the conserved domains involved in fidelity control (nsp14) and mRNA capping (nsp13–16).^{17,21} Figure 1B summarizes the reactions involved in capping newly synthesized viral mRNA (pppN-RNA).

The viral proteins responsible for RNA synthesis, proofreading, and capping (nsp7, -8, -10, -12–14, and -16) form the RTC core. The following mechanism to produce stable viral RNA has been proposed:^{20,21} First, a RNA template is unwound by nsp13 helicase and subsequently translocated to the nsp12 active site where a nascent ssRNA is synthesized.²⁰ The neighboring nsp14 excises any erroneous nucleotides from

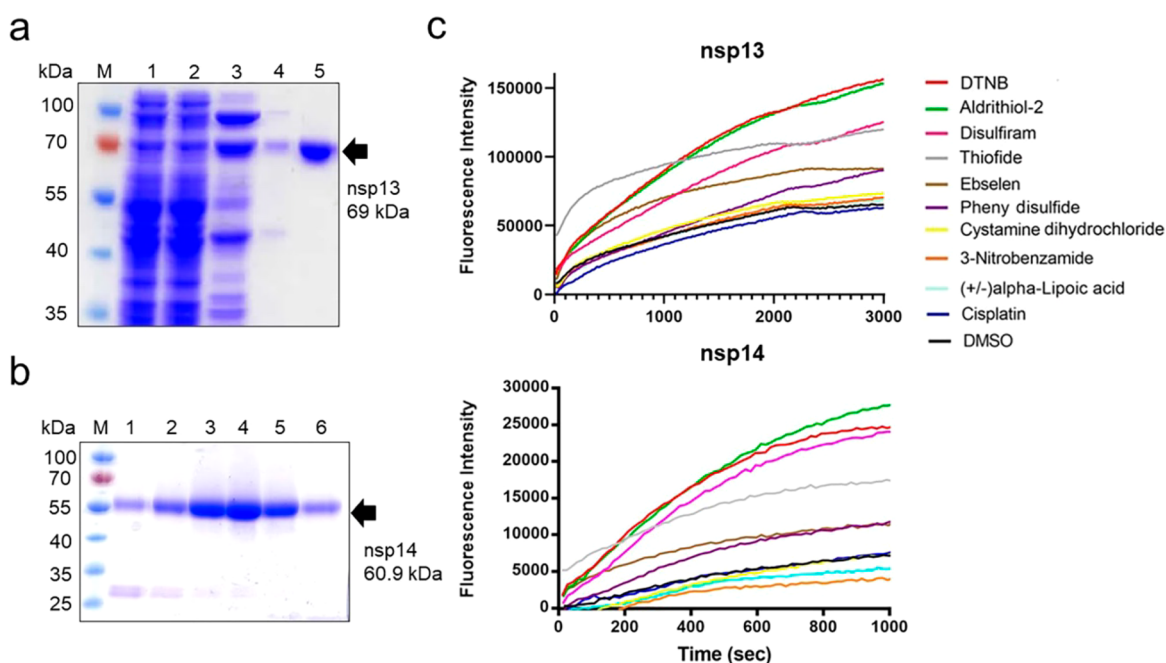


Figure 2. Zn²⁺ ions are released from SARS-CoV-2 nsp13 and nsp14 by Zn²⁺-ejecting compounds. (a) His-tagged nsp13 was purified to high homogeneity, as shown by SDS-PAGE. The final purified nsp13 (in lane 5) was used for Zn²⁺-ejecting and enzymatic assays. The protein marker (M), cell extract (lane 1), the flow through from the HisTrap FF column at different imidazole concentrations (lanes 2 and 3), and the flow through from the Hitrap SP HP column (in lanes 4) are shown, respectively. (b) Purified His-tagged nsp14 (lanes 3–6) had high homogeneity, as shown by SDS-PAGE. (c) nsp13 (5 μM) and nsp14 (5 μM) were each incubated with FluoZin-3 and one of the Zn²⁺-ejecting compounds (5 μM). The released Zn²⁺ ions were detected by the increase in the fluorescence signal from FluoZin-3 with excitation and emission wavelengths of 494 and 516 nm, respectively.

the nascent pppN-RNA, which is dephosphorylated by nsp13. An unknown GTase, nsp14, and nsp16 cap the viral ppN-RNA yielding m⁷GpppNm-RNA. nsp10, an allosteric activator of nsp14 and nsp 16, acts as a molecular connector between proofreading and capping activities.²¹ Because the RTC core is indispensable for SARS-CoV-2 replication, using clinically safe drugs to target its constituent proteins would reduce viral load.

Interestingly, the nsp3 PL^{pro} domain, nsp10 zinc-finger, nsp12, nsp13, and nsp14 possess several Zn²⁺ sites that are conserved among β-coronaviruses.²³ The Zn²⁺ sites in these nsps serve an essential structural role^{19,23–26} as well as a vital catalytic role for nsp13 helicase activity²⁶ and nsp14 ExoN exonuclease activity.²⁴ Among the multiple Zn²⁺ sites in SARS-CoV-2, the structural Zn²⁺ sites in nsp3 PL^{pro} and nsp10 have been found to be *labile*,²³ i.e., Zn²⁺ ions that contribute to structural stability are released upon reaction of the Zn²⁺-bound Cys thiolates with Zn²⁺-ejecting agents.^{27–30} However, it is not known whether the Zn²⁺ sites in nsp13 and nsp14, which constitute the RTC, are also labile and can be targeted by clinically safe Zn²⁺-ejector drugs such as disulfiram, an approved antialcoholic drug, and ebselen, in phase III clinical trials for hearing loss. To address this possibility, we have overexpressed SARS-CoV-2 nsp13 and nsp14 proteins to see if their Zn²⁺ ions could be ejected by Zn²⁺-ejecting agents and if clinically safe disulfiram and ebselen can inhibit their enzymatic activities. On the basis of the finding herein that the Zn²⁺-ejector drugs could indeed inhibit the enzymatic activities of SARS-CoV-2 nsp13 and nsp14, we further assessed if disulfiram/ebselen combined with remdesivir, which stops RNA synthesis, could synergistically inhibit SARS-CoV-2 replication.

RESULTS

Zn²⁺ Ions Are Released from SARS-CoV-2 nsp13 and nsp14 by Zn²⁺-Ejecting Agents. His-tagged full-length SARS-CoV-2 nsp13 and nsp14 were expressed in *Escherichia coli*, and the recombinant proteins were purified by chromatographic methods to a high homogeneity (Figure 2a,b). After incubating SARS-CoV-2 nsp13 and nsp14 with the Zn²⁺-specific fluorophore FluoZin-3 (1 μM), a Zn²⁺-ejecting compound (5 μM) was added. Ten Zn²⁺-ejecting compounds were tested: 2,2'-dithiobisbenzothiazole (also known as thiofide), cystamine dihydrochloride, 5,5'-dithiobis(2-nitrobenzoic acid) (DTNB), phenyl disulfide, 3-nitrobenzamide, tetraethylthiuram disulfide (disulfiram), 2,2'-dithiopyridine (aldrithiol-2), (±)alpha-lipoic acid, ebselen, and cisplatin. Release of Zn²⁺ ions was monitored by the increase of the fluorescence signal from FluoZin-3 (Figure 2c). Five of the Zn²⁺-ejecting compounds (DTNB, aldrithiol-2, disulfiram, thiofide, and ebselen) effectively ejected Zn²⁺ ions from the SARS-CoV-2 nsp13 and nsp14 proteins.

Disulfiram and Ebselen Inhibit SARS-CoV-2 nsp13 ATPase Activity. SARS-CoV-2 nsp13 consists of an N-terminal Zn²⁺-binding domain that is connected to an inserted domain (1B) by a stalk region and two RecA ATPase domains. These domains work together to complete the helicase unwinding function.^{26,31} The Zn²⁺-binding domain is not directly involved in unwinding double-stranded DNA/RNA, but nevertheless, it is critical for nsp13 helicase activity.³² Can the release of Zn²⁺ ions from SARS-CoV-2 nsp13 affect its helicase activity? To address this, we exploited the following: SARS-CoV-2 nsp13 is an NTP-dependent helicase, and its unwinding activity/helicase activity depends on ATPase activity.²⁶ Hence, we measured the ATPase activity of SARS-

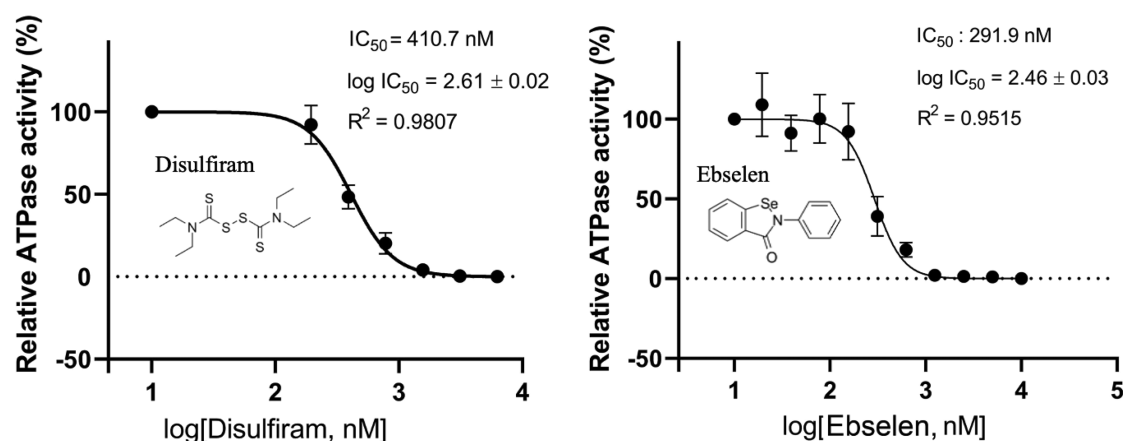


Figure 3. Inhibition of the ATPase activity of SARS-CoV-2 nsp13 by disulfiram and ebselen. The ATPase activity of SARS-CoV-2 nsp13 ($0.25 \mu\text{M}$) was estimated by measurement of the phosphate ion concentrations using the molybdenum blue method in the presence of $0.25 \mu\text{M}$ ssDNA and different concentrations of disulfiram (0.2 – $12.5 \mu\text{M}$) or ebselen (0.02 – $10.0 \mu\text{M}$). The half-maximal inhibitory activity (IC_{50}) of disulfiram and ebselen in inhibiting the ATPase activity of SARS-CoV-2 nsp13 is shown. Error bars shown in the two panels represent the standard errors from three replicates of the experiment.

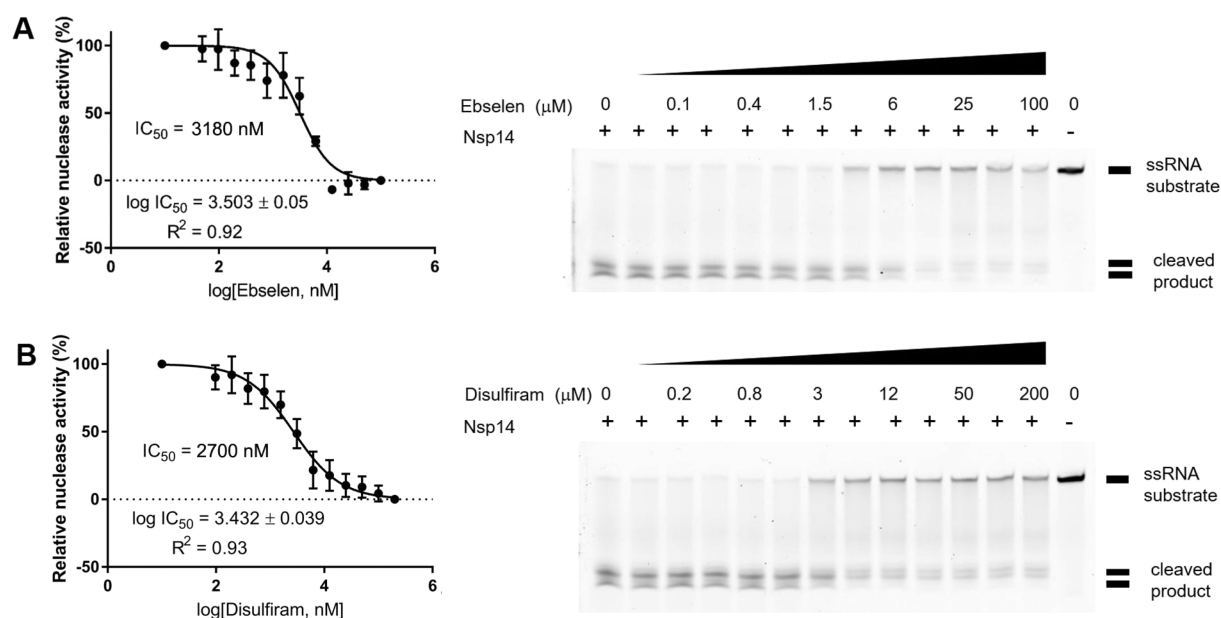


Figure 4. Inhibition of the exoribonuclease activity of SARS-CoV-2 nsp14 by ebselen and disulfiram. (A) SARS-CoV-2 nsp14 degraded the FAM-labeled 37-nucleotide ssRNA ($5'$ -FAM- C_7U_{30} - $3'$) into small fragments as revealed in the TBE gel (right panel). Increased concentrations of ebselen (0 – $100 \mu\text{M}$) gradually inhibited nsp14 exoribonuclease activity with an estimated IC_{50} of $3.18 \mu\text{M}$ (left panel). (B) Disulfiram inhibited the exoribonuclease activity of nsp14 with an estimated IC_{50} of $2.70 \mu\text{M}$. In the two gels, the relative nuclease activity (%) was estimated based on the band intensity of the cleaved products, normalized to that in the first lane (no drug, 100% activity) and that in the second to last lane corresponding to 0% activity with $100 \mu\text{M}$ ebselen or $200 \mu\text{M}$ disulfiram. Error bars shown in the two left panels represent the standard errors from three replicates of the experiment.

CoV-2 nsp13 by the molybdenum blue method³³ in the presence and absence of disulfiram/ebselen to examine if these Zn^{2+} -ejecting compounds can inhibit nsp13 enzymatic activity. The relative ATPase activities of nsp13 were estimated from the concentration of phosphate ions produced during ATP hydrolysis in the presence of single-stranded DNA and disulfiram (0.2 – $12.5 \mu\text{M}$) or ebselen (0.2 – $10.0 \mu\text{M}$) (Figure 3). The Zn^{2+} -ejecting assays in Figure 2c suggest that Zn^{2+} ions can be ejected comparably by disulfiram and ebselen after 10 min incubation with nsp13. We thus incubated nsp13 with disulfiram/ebselen for 10 min and then measured nsp13 ATPase activity. On the basis of the measurements, disulfiram and ebselen inhibited the ATPase activity of nsp13 with

comparable $\log \text{IC}_{50}$ values of 2.6 and 2.5 nM, respectively. The corresponding IC_{50} values indicate that ebselen ($\text{IC}_{50} = 291 \text{ nM}$) is slightly more potent than disulfiram ($\text{IC}_{50} = 410.7 \text{ nM}$), consistent with its slightly more efficient Zn^{2+} release from nsp 13 in the reaction time of 10 min (600 s , Figure 2c).

Disulfiram and Ebselen Inhibit SARS-CoV-2 nsp14 Exoribonuclease Activity. SARS-CoV nsp14 has two zinc-finger motifs (Zf1 and Zf2) in the ExoN domain responsible for proofreading and one zinc-finger motif (Zf3) in the N7-MTase domain involved in mRNA capping.²⁴ Truncating the C-terminal region of Zf3 disrupted local hydrophobic interactions, causing a decrease in the N7-MTase activity.²⁴ To see if release of Zn^{2+} cations from SARS-CoV-2 nsp14

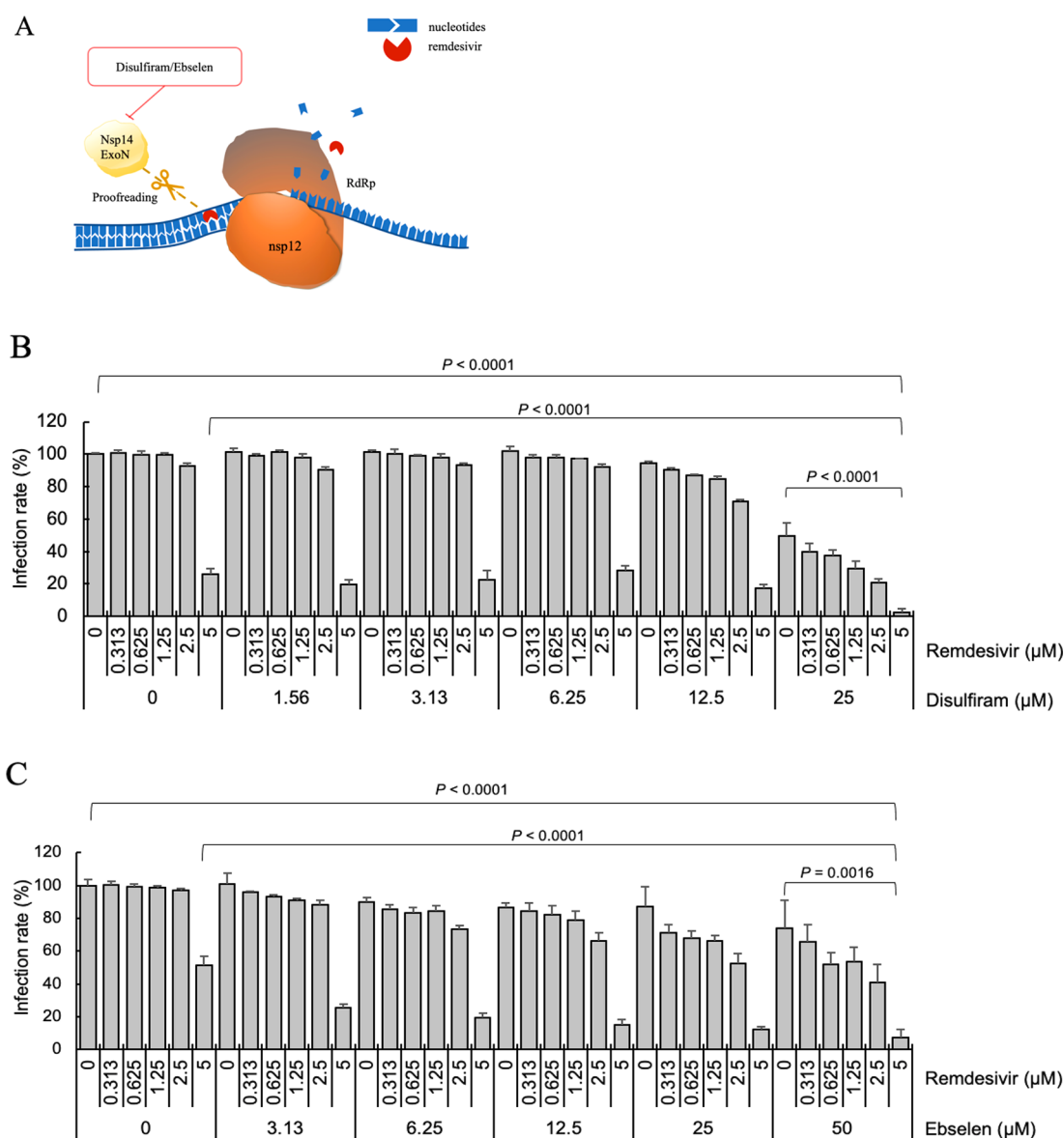


Figure 5. Antiviral potential of disulfiram/ebesen and remdesivir. (A) The active form of remdesivir inhibits nsp12 RdRp by competing with the natural ATP substrate. Disulfiram/ebesen can inhibit nsp14 ExoN proofreading activity, as shown above. The SARS-CoV-2 infection rates in Vero E6 cells treated with remdesivir and (B) disulfiram or (C) ebselen were determined and are shown as means and standard deviations ($n = 4$). The infection rate of no-compound treatment was set as 100%. The p values were calculated by t -test.

could inhibit its exoribonuclease function, we measured the 3′–5′ exoribonuclease activity of nsp14 in cleaving a 5′-end-fluorophore-labeled ssRNA (5′-FAM-C₇U₃₀-3′) in the presence and absence of the Zn²⁺-ejecting drugs. The 37-nucleotide ssRNA was degraded by nsp14 into small fragments. However, upon addition of ebselen (from 0 to 100 μM) or disulfiram (from 0 to 200 μM), the amount of cleaved RNA products was gradually reduced (Figure 4). The relative (%) nuclease activity with respect to different concentrations of a given Zn²⁺ ejector was calculated based on the band intensity of the cleaved products. This gave an estimated IC₅₀ of 3.18 μM for ebselen and 2.70 μM for disulfiram in inhibiting SARS-CoV-2 nsp14 exoribonuclease activity.

Disulfiram/Ebselen and Remdesivir Exhibit Synergistic Antiviral Activity. Remdesivir, an adenosine analog RdRp inhibitor, has gained emergency FDA approval to treat acute COVID-19 patients.^{9,34} It outcompetes the natural ATP

substrate for binding to nsp12 RdRp, and upon RNA chain elongation, its cyano (CN) group has steric clashes with RdRp, inducing delayed chain termination.^{34–36} Although remdesivir is better than other nucleotide analogs in avoiding removal by the proofreading nsp14 ExoN, it may still be removed by nsp14, as it is more effective in a model β-coronavirus (murine hepatitis virus) lacking the proofreading ExoN activity compared to that of the wild-type virus, as well as in viral mutants with reduced exonuclease activity.^{37,38} Indeed, remdesivir has shown only moderate success in clinical studies: The ACTT-1 trial³⁹ reported that remdesivir moderately reduced time to recovery, but the WHO SOLIDARITY trial did not.⁴⁰ Mortality results from four trials of remdesivir suggested some benefit in only low-risk patients.⁴⁰

We hypothesize that inhibition of SARS-CoV-2 proofreading activity by disulfiram/ebesen may allow remdesivir to escape nsp14 ExoN-mediated removal; thus, combining remdesivir with disulfiram/ebesen may help to improve inhibition of viral

RNA synthesis (Figure 5A).⁴¹ To see if remdesivir combined with disulfiram/ebesen could exhibit synergistic inhibition of SARS-CoV-2 replication, Vero E6 cells were treated with a given concentration of remdesivir and/or disulfiram/ebesen (Figures S1A and S2A). Figure 5B,C shows the SARS-CoV-2 infection rate as the mean and corresponding standard deviation of four replicates. Disulfiram/ebesen combined with remdesivir exhibited enhanced antiviral effect compared to each drug alone with p values < 0.05.

To quantify the synergistic antiviral effect, the synergy score between two drugs was calculated using the SynergyFinder.⁴² As there are different reference models for quantifying degrees of synergy and their synergy scores may sometimes disagree, we used several well-known models that are based on different assumptions (dose–response-independent scores, HSA and Bliss, and dose–response-dependent scores, ZIP).⁴³ All models gave consistent results; hence, we report the ZIP score below. To make our prediction robust, we consider interaction between two drugs to be synergetic if the average ZIP score is >10, i.e., >10% of response beyond expectation, antagonistic if it is < -10, and additive if it is between -10 and 10. The ZIP scores between disulfiram and remdesivir are ≥ 0 for all concentrations with a mean of 11.4 for the most synergistic area and a maximum of 23.7, indicating synergistic interaction (Figure S1B). The ZIP scores between ebesen and remdesivir are also ≥ 0 for all concentrations; its average value for the most synergistic area is 24.6 with a maximum of 32.7, indicating synergistic interaction (Figure S2B). The results verify that remdesivir combined with disulfiram/ebesen show synergistic SARS-CoV-2 inhibition, and the synergy is greater when doses of the drug pair are increased.

DISCUSSION

The RTC core, which plays critical roles in SARS-CoV-2 replication as well as evasion of nucleoside analog drugs and innate immune responses, is evidently an important drug target. To date, drugs have been developed/repurposed to target a specific component of this complex such as nsp12 RdRp.^{3,44} In sharp contrast, we employ clinically safe Zn²⁺-ejector drugs to target *multiple conserved sites* in the RTC core. We show that disulfiram/ebesen can target conserved Zn²⁺ sites in nsp13 and nsp14, and their combination with remdesivir can synergistically inhibit SARS-CoV-2 replication in Vero E6 cells. We propose the following mechanism for the observed effects: By ejecting Zn²⁺ from the nsp13 Zn²⁺-binding domain, which is crucial for helicase and triphosphatase activities and interactions with nsp12,^{26,31} disulfiram/ebesen not only inhibits nsp13 enzymatic activities but also may disrupt nsp12–nsp13 interactions and affect nsp12 RdRp-catalyzed synthesis of viral RNA. It may also affect virus–host interactions since many human proteins involved in organization of the centrosome and Golgi, transcriptional regulation, protein kinase A and immune signaling, and vesicle trafficking have been identified as interacting with nsp13 using affinity purification of 26 SARS-CoV-2 proteins followed by mass spectrometry.⁴⁵ Notably, nsp13 targets innate immune signaling proteins along the interferon and nuclear factor- κ B (NF- κ B) pathways.^{45,48} By ejecting “structural” Zn²⁺ ions from the nsp14 ExoN domain, disulfiram/ebesen can inhibit SARS-CoV-2 nsp14 exoribonuclease activity. This would mitigate the efficacy of nsp14 to excise erroneous nucleotides and allow nucleotide/nucleoside analog drugs such as remdesivir to inhibit viral RNA synthesis. In addition to nsp13 and nsp14,

disulfiram/ebesen can also eject “structural” Zn²⁺ from the conserved nsp10 zinc finger domain,²³ which would destabilize the nsp10–nsp14–nsp16 complex that is essential for mRNA capping (see Figure 1).^{17,47,48} This would allow the host’s antiviral sensors to detect viral uncapped RNA, which can be degraded, and to prevent the virus from evading host immune responses.

Altogether, this work and previous studies show that disulfiram/ebesen can target *multiple conserved sites* in the viral RTC that are crucial for SARS-CoV-2 RNA genome replication as well as translation of the viral proteins (Figure 1). It can destabilize nsp10 cofactor,²³ a crucial mediator of protein–protein interactions, and inhibit the enzyme activities of nsp3 PL^{pro},²³ nsp5 M^{pro},⁶ nsp13, and nsp14, and probably nsp12 and nsp16 through their interactions with nsp13 and nsp10–nsp14, respectively. Disulfiram/ebesen can target not only the Zn²⁺-bound cysteines but also catalytic cysteines²³ and thereby inhibit SARS-CoV-2 M^{pro},⁶ which does not possess a Zn²⁺-site. By inhibiting M^{pro} and PL^{pro} viral proteolysis, disulfiram/ebesen can prevent efficient cleavage of the replicase polyproteins into component nsps. In case the virus produces resistance against these proteases, disulfiram/ebesen can also inhibit the RTC core that is crucial for viral RNA synthesis, proofreading, and capping, thus restoring remdesivir’s ability to function as a delayed chain terminator. As SARS-CoV-2 nsp3, nsp5, nsp13, and nsp14 enzymes target the interferon and/or NF- κ B pathway,^{45,46} their inhibition by disulfiram/ebesen may help to restore innate immune responses.

Unlike most studies that target a specific viral protein such as M^{pro}^{5,6} or the spike protein^{1,2} by developing potent (nanomolar) inhibitors or antibodies, our strategy simultaneously targets *multiple conserved viral proteins* responsible for viral polypeptide proteolysis as well as viral genome replication and viral protein translation using clinically safe Zn²⁺-ejector drugs. This has several advantages: Whereas a single viral drug target such as M^{pro} or the spike protein can undergo mutations to produce resistance against specific drugs, it would be less likely for the *multiple conserved viral proteins* that are jointly responsible for viral replication and transcription to simultaneously mutate and achieve drug resistance. Mutations of the conserved Zn²⁺-binding cysteines in nsp3, nsp10, and nsp12–14 that are targeted by disulfiram/ebesen would likely disrupt binding to Zn²⁺ cations that serve essential structural and/or catalytic roles in several SARS-CoV-2 proteins. Furthermore, disulfiram/ebesen targets the “upstream” part of the SARS-CoV-2 life cycle (Figure 1) before multiple replicated viruses leave the infected cell. Importantly, disulfiram is inexpensive, widely available, and easily administered, and may allow other broad-spectrum antivirals to synergistically inhibit a new virus, as shown herein. A third advantage is that our strategy is not specific to a particular SARS-CoV-2 variant or any type of coronavirus. This is because the proteins essential for RNA replication such as the RTC core are the most conserved among coronaviruses. Indeed, analysis of the SARS-CoV-2 gene sequences show the least divergence in the gene encoding these conserved domains (<https://nextstrain.org/ncov/global>). Thus, our approach may prove useful not only for the current COVID-19 pandemic but also in future coronavirus outbreaks where it may be deployed as a first line of defense in the absence of monoclonal antibodies and vaccines.

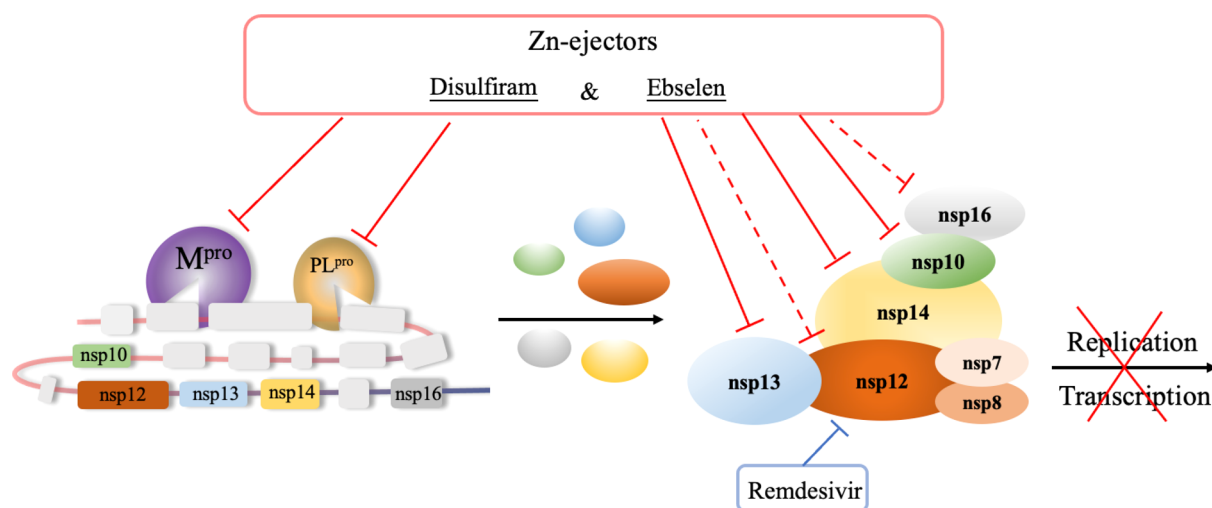


Figure 6. Disulfiram and ebselen can target multiple SARS-CoV-2 nsps to block the viral polyprotein cleavage and RNA replication/transcription. These Zn^{2+} -ejector drugs target PL^{pro} of nsp3 and M^{pro} of nsp5 to inhibit viral polypeptide proteolysis. They also directly target nsp10, nsp13, and nsp14 as well as indirectly target nsp12 and nsp16 to inhibit viral RNA genome replication and translation of the structural and accessory viral proteins. They can act in concert with remdesivir to synergistically inhibit SARS-CoV-2 replication.

In summary, we show that clinically safe Zn^{2+} -ejector drugs (disulfiram/ebselen) can target conserved functionally important Zn^{2+} sites in the multiprotein RTC and, when combined with remdesivir, that these can synergistically inhibit SARS-CoV-2 replication in Vero E6 cells (Figure 6).

EXPERIMENTAL SECTION

Protein Expression and Purification. The cDNA of SARS-CoV-2 nsp13 (residues 5302–5902 of pp1a/pp1ab) and nsp14 (residues 5903–6429 pp1a/pp1ab) were synthesized from Protech, Inc. (Taiwan) and cloned into pET28a and pRSFDuet-1 vectors, respectively, for expression of the N-terminal His-tagged nsp13 and the C-terminal His-tagged nsp14. Both plasmids were transformed into *E. coli* BL21 (DE3) pLysS strain cultured in LB medium supplemented with 50 $\mu\text{g}/\text{mL}$ kanamycin. Cells were grown to an optical density of 0.6 measured at a wavelength of 600 nm and induced by 0.2 mM IPTG at 18 °C for 14–16 h to express His-tagged SARS-CoV-2 nsp13 and nsp14.

The harvested cells expressing nsp13 were disrupted by a microfluidizer (Microfluidics M-110P) in lysis buffer containing 50 mM Tris-HCl (pH 8.0), 500 mM NaCl, protease inhibitor, 5% glycerol, and 10 mM β -mercaptoethanol. The supernatant was run through a HisTrap FF column (5 mL, GE HealthCare) and washed with a washing buffer containing 50 mM Tris-HCl (pH 8.0), 200 mM NaCl, 5% glycerol, and 30 mM imidazole. The eluted nsp13 was further purified by a HiTrap SP HP column (5 mL, GE HealthCare) to produce a homogeneous nsp13 protein sample.

For the purification of nsp14, the harvested cells were resuspended in lysis buffer (20 mM HEPES (pH 7), 150 mM NaCl, 4 mM MgCl_2 , 5% glycerol, and 10 mM β -mercaptoethanol). After homogenization, the supernatant was loaded into a HisTrap FF column (5 mL, GE HealthCare) and washed with a washing buffer containing 20 mM HEPES (pH 7.0), 150 mM NaCl, 4 mM MgCl_2 , 5% glycerol, 10 mM β -mercaptoethanol, and 40 mM imidazole. The protein sample was collected and further loaded into a gel filtration column (HiLoad 16/60 Superdex 200, GE HealthCare), then eluted by

a buffer of 50 mM HEPES (pH 7.4), 50 mM NaCl, 5 mM MgCl_2 , and 5% glycerol.

Zn^{2+} -Ejection Assays. Zn^{2+} -ejecting agents were purchased from Sigma-Aldrich (USA), including 2,2'-dithiobis(benzothiazole), cystamine dihydrochloride, 5,5'-dithiobis(2-nitrobenzoic acid) (DTNB), phenyl disulfide, 3-nitrobenzamide, tetraethylthiuram disulfide (disulfiram), 2,2'-dithiodipyridine, (\pm)alpha-lipoic acid, ebselen, and cisplatin. The Zn^{2+} -specific fluorophore FluoZinTM-3 (Invitrogen/Life Technologies) was used to monitor the release of Zn^{2+} ions from SARS-CoV-2 nsp13 and nsp14. The Zn^{2+} -ejecting agents were dissolved in DMSO to a stock solution of 100 μM . SARS-CoV-2 His-tagged nsp13 (5 μM) and nsp14 (5 μM) were respectively mixed with each Zn^{2+} -ejecting agent (5 μM) and FluoZin-3 (1 μM) in a total reaction volume of 200 μL at room temperature. Fluorescence emission was then measured by EnSpire Multilabel Plate Reader (PerkinElmer, USA) at an excitation wavelength of 494 nm and emission wavelength of 516 nm.

Inhibition of the nsp13 ATPase Activity by Zn^{2+} Ejector Drugs. ATPase activity of SARS-CoV-2 nsp13 was analyzed by the molybdenum blue method³³ to measure the phosphate ion concentration in ATP hydrolysis reaction in the presence of the Zn^{2+} ejector drugs disulfiram and ebselen. nsp13 (2.5 μM , 10 μL) was mixed with or without disulfiram (2–125 μM , 10 μL) or ebselen (0.2–100 μM , 10 μL) in 60 μL of the reaction buffer containing 33 mM Tris-HCl (pH 8.0) and 5 mM MgCl_2 at room temperature for 10 min. ATP (50 mM, 10 μL) and ssDNA (2.5 μM , 10 μL) with a sequence of 5'-(dT)₂₄-3' were then added into the nsp13 solution and incubated for 10 min. The ATPase reaction was stopped by adding 100 μL of 10% SDS, and the blue complexes between inorganic phosphate and molybdate were developed by adding 100 μL of 1.25% ammonium molybdate in 6.5% sulfuric solution and 100 μL of freshly prepared 10% (*w/v*) ascorbic acid. A total of 400 μL of reaction solution was incubated at 25 °C for 10 min and then read at 660 nm by Enspire plate reader (PerkinElmer). Various concentrations of Na_2HPO_4 ranging from 0.05 to 0.5 mM were also prepared as a standard curve. The relative ATPase activity of SARS-CoV-2 nsp13 in the

presence of each Zn²⁺ ejector was compared to that without adding Zn²⁺ ejector, and the half-maximal inhibitory activity (IC₅₀) of each inhibitor was calculated by GraphPad Prism.

Inhibition of the nsp14 Exoribonuclease Activity by Zn²⁺ Ejector Drugs. nsp14 (50 μM, 100 μL) was mixed with 4 μL of 5'-end FAM-labeled ssRNA (1 μM, 5'-FAM-C₇U₃₀-3') in 200 μL of the reaction buffer (100 mM HEPES (pH 7.4), 100 mM NaCl, 10 mM MgCl₂ and 10% glycerol), and 100 μL of ddH₂O. Disulfiram (1 μL, 0–200 μM) or ebselen (1 μL, 0–100 μM) in different concentrations was then added to the nsp14 and RNA mixture (19 μL), and incubated for 30 min at 37 °C. The RNA loading dye (20 μL, 89 mM Tris-HCl, pH 8, 89 mM boric acid, 2 mM EDTA, 0.01% bromophenol blue, 0.02% xylene cyanol FF, and 7 M urea) was then added into the mixture, and the sample was heated at 95 °C for 5 min to stop the reaction. The RNA in the mixtures were separated on TBE gel and visualized by Biomolecular Imager (Amersham Typhoon, GE HealthCare). The resolved RNA bands in the gel were analyzed by ImageJ, and the IC₅₀ of each inhibitor was calculated by GraphPad Prism.

Cell-Based Assays. Remdesivir was produced following the previous protocol.⁴⁹ Vero E6 cells were pretreated with the disulfiram/ebselen and/or remdesivir at various concentrations for 1 h at 37 °C and then adsorbed with SARS-CoV-2 TCDC#4 (hCoV-19/Taiwan/4/2020) at MOI 0.005 (100 PFU/well) for 1 h at 37 °C. After virus adsorption, the cells were replenished with fresh medium and compounds at the indicated concentrations for 1 day of incubation. The cells were fixed with 10% formaldehyde, permeabilized with 0.5% Triton X-100, and stained with anti-SARS-CoV-2 N protein antibody (provided by Dr. An-Suei Yang, Genomic Research Center, Academia Sinica, Taiwan) and anti-human IgG-488. The N protein expression was measured using a high-content image analysis system (Molecular Devices), and the average infection rate of no-drug treatment was set as 100%. The synergy score is calculated using the SynergyFinder to quantify the synergistic antiviral effect between disulfiram/ebselen and remdesivir.

■ ASSOCIATED CONTENT

Supporting Information

The Supporting Information is available free of charge at <https://pubs.acs.org/doi/10.1021/acspsci.1c00022>.

Synergistic antiviral potential of disulfiram with remdesivir, and synergistic antiviral potential of ebselen with remdesivir (PDF)

■ AUTHOR INFORMATION

Corresponding Authors

Carmay Lim – Institute of Biomedical Sciences, Academia Sinica, Taipei 115, Taiwan; Department of Chemistry, National Tsing Hua University, Hsinchu 300, Taiwan; orcid.org/0000-0001-9077-7769; Email: carmay@gate.sinica.edu.tw

Hanna S. Yuan – Institute of Molecular Biology, Academia Sinica, Taipei 115, Taiwan; Email: hanna@sinica.edu.tw

Authors

Ting Chen – Institute of Biomedical Sciences, Academia Sinica, Taipei 115, Taiwan; orcid.org/0000-0001-8055-3104

Cheng-Yin Fei – Institute of Molecular Biology, Academia Sinica, Taipei 115, Taiwan

Yi-Ping Chen – Institute of Molecular Biology, Academia Sinica, Taipei 115, Taiwan

Karen Sargsyan – Institute of Biomedical Sciences, Academia Sinica, Taipei 115, Taiwan

Chun-Ping Chang – Institute of Biotechnology and Pharmaceutical Research, National Health Research Institutes, Miaoli 350, Taiwan; orcid.org/0000-0003-1424-5546

Complete contact information is available at: <https://pubs.acs.org/10.1021/acspsci.1c00022>

Notes

The authors declare no competing financial interest.

■ ACKNOWLEDGMENTS

The cell-based experiments were performed by Dr. Jian-Jong Liang (jjliang1234@yahoo.com.tw) and Dr. Chun-Che Liao (jfliao@ibms.sinica.edu.tw) in Dr. Yi-Ling Lin's laboratory at the Institute of Biomedical Sciences (IBMS), Academia Sinica, Taipei, Taiwan. We thank Taiwan CDC for providing SARS-CoV-2 TCDC#4 (hCoV-19/Taiwan/4/2020) and funding support from Academia Sinica for IBMS P3 facility (AS-CFII-108-102) and the Ministry of Science and Technology, Taiwan for COVID-19 study (MOST 109-3114-Y-001-001). We thank Dr. Karine Mazmanian for help with the figures. We acknowledge the DNA Sequencing Core Facility (IBMS, AS-CFII-108-115) of the Scientific Instrument Center in Academia Sinica for DNA sequencing. This work was supported by the Ministry of Science & Technology (MOST-107-2113-M-001-018 to C.L.) and Academia Sinica (AS-IA-107-L03 to C. L. and AS-IA-110-L02 to H.S.Y.) Taiwan.

■ REFERENCES

- (1) Kim, P. S., Read, S. W., and Fauci, A. S. (2020) Therapy for early COVID-19: A critical need. *JAMA* 324, 2149–2150.
- (2) Chen, P., Nirula, A., Heller, B., Gottlieb, R. L., Boscia, J., Morris, J., Huhn, G., Cardona, J., Mocherla, B., Stosor, V., et al. (2021) SARS-CoV-2 neutralizing antibody LY-CoV555 in outpatients with Covid-19. *N. Engl. J. Med.* 384, 229–237.
- (3) Zhou, Q. A., Kato-Weinstein, J., Li, Y., Deng, Y., Granet, R., Garner, L., Liu, C., Polshakov, D., Gessner, C., and Watkins, S. (2020) Potential therapeutic agents and associated bioassay data for COVID-19 and related human coronavirus infections. *ACS Pharmacol. Transl. Sci.* 3, 813–834.
- (4) Wrapp, D., Wang, N., Corbett, K. S., Goldsmith, J. A., Hsieh, C.-L., Abiona, O., Graham, B. S., and McLellan, J. S. (2020) Cryo-EM structure of the 2019-nCoV spike in the prefusion conformation. *Science* 367, 1260–1263.
- (5) Zhang, L., Lin, D., Sun, X., Curth, U., Drosten, C., Sauerhering, L., Becker, S., Rox, K., and Hilgenfeld, R. (2020) Crystal structure of SARS-CoV-2 main protease provides a basis for design of improved α -ketoamide inhibitors. *Science* 368, 409–412.
- (6) Jin, Z., Du, X., Xu, Y., Deng, Y., Liu, M., Zhao, Y., Zhang, B., Li, X., Zhang, L., Peng, C., Duan, Y., Yu, J., Wang, L., Yang, K., Liu, F., Jiang, R., Yang, X., You, T., Liu, X., Yang, X., Bai, F., Liu, H., Liu, X., Guddat, L. W., Xu, W., Xiao, G., Qin, C., Shi, Z., Jiang, H., Rao, Z., and Yang, H. (2020) Structure of M^{pro} from COVID-19 virus and discovery of its inhibitors. *Nature* 582, 289–293.
- (7) Maiti, B. K. (2020) Can papain-like protease inhibitors halt SARS-CoV-2 replication? *ACS Pharmacol. Transl. Sci.* 3, 1017–1019.
- (8) Gao, Y., Yan, L., Huang, Y., Liu, F., Zhao, Y., Cao, L., Wang, T., Sun, Q., Ming, Z., Zhang, L., Ge, J., Zheng, L., Zhang, Y., Wang, H.,

- Zhu, Y., Zhu, C., Hu, T., Hua, T., Zhang, B., Yang, X., Li, J., Yang, H., Liu, Z., Xu, W., Guddat, L. W., Wang, Q., Lou, Z., and Rao, Z. (2020) Structure of the RNA-dependent RNA polymerase from COVID-19 virus. *Science* 368, 779–782.
- (9) Yin, W., Mao, C., Luan, X., Shen, D.-D., Shen, Q., Su, H., Wang, X., Zhou, F., Zhao, W., Gao, M., et al. (2020) Structural basis for inhibition of the RNA-dependent RNA polymerase from SARS-CoV-2 by remdesivir. *Science* 368, 1499–1504.
- (10) Starr, T. N., Greaney, A. J., Addetia, A., Hannon, W. W., Choudhary, M. C., Dingens, A. S., Li, J. Z., and Bloom, J. D. (2021) Prospective mapping of viral mutations that escape antibodies used to treat COVID-19. *Science* 371, 850–854.
- (11) McCarthy, K. R., Rennick, L. J., Nambulli, S., Robinson-McCarthy, L. R., Bain, W. G., Haidar, G., and Duprex, W. P. (2021) Recurrent deletions in the SARS-CoV-2 spike glycoprotein drive antibody escape. *Science* 371, 1139.
- (12) Matheson, N. J., and Lehner, P. J. (2020) How does SARS-CoV-2 cause COVID-19? *Science* 369, 510–511.
- (13) Coronaviridae Study Group of the International Committee on Taxonomy of Viruses (2020) The species Severe acute respiratory syndrome-related coronavirus: classifying 2019-nCoV and naming it SARS-CoV-2. *Nat. Microbiol.* 5, 536–544.
- (14) Wang, K., Chen, W., Zhang, Z., Deng, Y., Lian, J.-Q., Du, P., Wei, D., Zhang, Y., Sun, X.-X., Gong, L., et al. (2020) CD147-spike protein is a novel route for SARS-CoV-2 infection to host cells. *Signal Transduct. Target. Ther.* 5, 283.
- (15) Letko, M., Marzi, A., and Munster, V. (2020) Functional assessment of cell entry and receptor usage for SARS-CoV-2 and other lineage B betacoronaviruses. *Nat. Microbiol.* 5, 562–569.
- (16) Hoffmann, M., Kleine-Weber, H., Schroeder, S., Krüger, N., Herrler, T., Erichsen, S., Schiergens, T. S., Herrler, G., Wu, N.-H., Nitsche, A., et al. (2020) SARS-CoV-2 cell entry depends on ACE2 and TMPRSS2 and is blocked by a clinically proven protease inhibitor. *Cell* 181, 271–280.
- (17) Snijder, E. J., Decroly, E., and Ziebuhr, J. (2016) The nonstructural proteins directing coronavirus RNA synthesis and processing. *Adv. Virus Res.* 96, 59–126.
- (18) V'kovski, P., Kratzel, A., Steiner, S., Stalder, H., and Thiel, V. (2021) Coronavirus biology and replication: implications for SARS-CoV-2. *Nat. Rev. Microbiol.* 19, 155–170.
- (19) Kirchdoerfer, R. N., and Ward, A. B. (2019) Structure of the SARS-CoV nsp12 polymerase bound to nsp7 and nsp8 co-factors. *Nat. Commun.* 10, 2342.
- (20) Yan, L., Zhang, Y., Ge, J., Zheng, L., Gao, Y., Wang, T., Jia, Z., Wang, H., Huang, Y., Li, M., et al. (2020) Architecture of a SARS-CoV-2 mini replication and transcription complex. *Nat. Commun.* 11, 5874.
- (21) Romano, M., Ruggiero, A., Squeglia, F., Maga, G., and Berisio, R. (2020) A structural view of SARS-CoV-2 RNA replication machinery: RNA synthesis, proofreading and final capping. *Cells* 9, 1267.
- (22) Bouvet, M., Lugari, A., Posthuma, C. C., Zevenhoven, J. C., Bernard, S., Betzi, S., Imbert, I., Canard, B., Guillemot, J. C., Lécine, P., Pfeifferle, S., Drosten, C., Snijder, E. J., Decroly, E., and Morelli, X. (2014) Coronavirus Nsp10, a critical co-factor for activation of multiple replicative enzymes. *J. Biol. Chem.* 289, 25783–25796.
- (23) Sargsyan, K., Lin, C. C., Chen, T., Grauffel, C., Chen, Y. P., Yang, W. Z., Yuan, H. S., and Lim, C. (2020) Multi-targeting of functional cysteines in multiple conserved SARS-CoV-2 domains by clinically safe Zn-ejectors. *Chem. Sci.* 11, 9904–9909.
- (24) Ma, Y., Wu, L., Shaw, N., Gao, Y., Wang, J., Sun, Y., Lou, Z., Yan, L., Zhang, R., and Rao, Z. (2015) Structural basis and functional analysis of the SARS coronavirus nsp14–nsp10 complex. *Proc. Natl. Acad. Sci. U. S. A.* 112, 9436–9441.
- (25) Hao, W., Wojdyla, J. A., Zhao, R., Han, R., Das, R., Zlatev, I., Manoharan, M., Wang, M., and Cui, S. (2017) Crystal structure of Middle East respiratory syndrome coronavirus helicase. *PLoS Pathog.* 13, No. e1006474.
- (26) Jia, Z., Yan, L., Ren, Z., Wu, L., Wang, J., Guo, J., Zheng, L., Ming, Z., Zhang, L., Lou, Z., and Rao, Z. (2019) Delicate structural coordination of the Severe Acute Respiratory Syndrome coronavirus Nsp13 upon ATP hydrolysis. *Nucleic Acids Res.* 47, 6538–6550.
- (27) Huang, M., Maynard, A., Turpin, J. A., Graham, L., Janini, G. M., Covell, D. G., and Rice, W. G. (1998) Anti-HIV agents that selectively target retroviral nucleocapsid protein zinc fingers without affecting cellular zinc finger proteins. *J. Med. Chem.* 41, 1371–1381.
- (28) Briknarova, K., Thomas, C. J., York, J., and Nunberg, J. H. (2011) Structure of a zinc-binding domain in the Junin virus envelope glycoprotein. *J. Biol. Chem.* 286, 1528–1536.
- (29) Lee, Y. M., Lin, Y. F., and Lim, C. (2014) Factors controlling the role of Zn and reactivity of Zn-bound cysteines in proteins: Application to drug target discovery. *J. Chin. Chem. Soc.* 61, 142–150.
- (30) Lee, Y. M., Duh, Y., Wang, S. T., Lai, M. M. C., Yuan, H. S., and Lim, C. (2016) Using an old drug to target a new drug site: Application of disulfiram to target the Zn-site in HCV NSSA protein. *J. Am. Chem. Soc.* 138, 3856–3862.
- (31) Chen, J., Malone, B., Llewellyn, E., Grasso, M., Shelton, P. M., Olinares, P. D. B., Maruthi, K., Eng, E. T., Vatandaslar, H., Chait, B. T., et al. (2020) Structural basis for helicase-polymerase coupling in the SARS-CoV-2 replication-transcription complex. *Cell* 182, 1560–1573.
- (32) Seybert, A., Posthuma, C. C., Van Dinten, L. C., Snijder, E. J., Gorbalenya, A. E., and Ziebuhr, J. (2005) A complex zinc finger controls the enzymatic activities of nidovirus helicases. *J. Virol.* 79, 696–704.
- (33) He, Z., and Honeycutt, C. W. (2005) A modified molybdenum blue method for orthophosphate determination suitable for investigating enzymatic hydrolysis of organic phosphates. *Commun. Soil Sci. Plant Anal.* 36, 1373–1383.
- (34) Eastman, R. T., Roth, J. S., Brimacombe, K. R., Simeonov, A., Shen, M., Patnaik, S., and Hall, M. D. (2020) Remdesivir: A review of its discovery and development leading to emergency use authorization for treatment of COVID-19. *ACS Cent. Sci.* 6, 672–683.
- (35) Badgular, K. C., Ram, A. H., Zanzay, R., Kadam, H., and Badgular, V. C. (2020) Remdesivir for COVID-19: A review of pharmacology, mechanism of action, in-vitro activity and clinical use based on available case studies. *J. Drug Delivery Ther.* 10, 264–270.
- (36) Gordon, C. J., Tchesnokov, E. P., Woolner, E., Perry, J. K., Feng, J. Y., Porter, D. P., and Gotte, M. (2020) Remdesivir is a direct-acting antiviral that inhibits RNA-dependent RNA polymerase from severe acute respiratory syndrome coronavirus 2 with high potency. *J. Biol. Chem.* 295, 6785–6797.
- (37) Agostini, M. L., Andres, E. L., Sims, A. C., Graham, R. L., Sheahan, T. P., Lu, X., Smith, E. C., Case, J. B., Feng, J. Y., Jordan, R., et al. (2018) Coronavirus susceptibility to the antiviral remdesivir (GS-5734) is mediated by the viral polymerase and the proofreading exoribonuclease. *mBio* 9, No. e00221-18.
- (38) Bravo, J., Dangerfield, T. L., Taylor, D. W., and Johnson, K. A. (2021) Remdesivir is a Delayed Translocation Inhibitor of SARS CoV-2 Replication. *Mol. Cell.* 35.
- (39) Beigel, J. H., Tomashek, K. M., Dodd, L. E., Mehta, A. K., Zingman, B. S., Kalil, A. C., Hohmann, E., Chu, H. Y., Luetkemeyer, A., Kline, S., et al. (2020) Remdesivir for the treatment of Covid-19—final report. *N. Engl. J. Med.* 383, 1813–1826.
- (40) WHO Solidarity Trial Consortium (2020) Repurposed antiviral drugs for COVID-19—interim WHO SOLIDARITY trial results. *N. Engl. J. Med.* 384, 497–511.
- (41) Shannon, A., Le, N. T. T., Selisko, B., Eydoux, C., Alvarez, K., Guillemot, J.-C., Decroly, E., Peersen, O., Ferron, F., and Canard, B. (2020) Remdesivir and SARS-CoV-2: Structural requirements at both nsp12 RdRp and nsp14 Exonuclease active sites. *Antiviral Res.* 178, 104793.
- (42) Ianevski, A., Giri, A. K., and Aittokallio, T. (2020) SynergyFinder 2.0: visual analytics of multi-drug combination synergies. *Nucleic Acids Res.* 48, W488–W493.
- (43) Vlot, A. H., Aniceto, N., Menden, M. P., Ulrich-Merzenich, G., and Bender, A. (2019) Applying synergy metrics to combination

screening data: agreements, disagreements and pitfalls. *Drug Discovery Today* 24, 2286–2298.

(44) Li, G., and De Clercq, E. (2020) Therapeutic options for the 2019 novel coronavirus (2019-nCoV). *Nat. Rev. Drug Discovery* 19, 149–150.

(45) Gordon, D. E., Jang, G. M., Bouhaddou, M., Xu, J., Obernier, K., White, K. M., O'Meara, M. J., Rezelj, V. V., Guo, J. Z., and Swaney, D. L. (2020) A SARS-CoV-2 protein interaction map reveals targets for drug repurposing. *Nature* 583, 459–468.

(46) Lei, X., Dong, X., Ma, R., Wang, W., Xiao, X., Tian, Z., Wang, C., Wang, Y., Li, L., Ren, L., et al. (2020) Activation and evasion of type I interferon responses by SARS-CoV-2. *Nat. Commun.* 11, 3810.

(47) Decroly, E., Debarnot, C., Ferron, F., Bouvet, M., Coutard, B., Imbert, I., Gluais, L., Papageorgiou, N., Sharff, A., Bricogne, G., Ortiz-Lombardia, M., Lescar, J., and Canard, B. (2011) Crystal structure and functional analysis of the SARS-coronavirus RNA cap 2'-O-methyltransferase nsp10/nsp16 complex. *PLoS Pathog.* 7, No. e1002059.

(48) Pruijssers, A. J., and Denison, M. R. (2019) Nucleoside analogues for the treatment of coronavirus infections. *Curr. Opin. Virol.* 35, 57–62.

(49) Siegel, D., Hui, H. C., Doerffler, E., Clarke, M. O., Chun, K., Zhang, L., Neville, S., Carra, E., Lew, W., Ross, B., Wang, Q., Wolfe, L., Jordan, R., Soloveva, V., Knox, J., Perry, J., Perron, M., Stray, K. M., Barauskas, O., Feng, J. Y., Xu, Y., Lee, G., Rheingold, A. L., Ray, A. S., Bannister, R., Strickley, R., Swaminathan, S., Lee, W. A., Bavari, S., Cihlar, T., Lo, M. K., Warren, T. K., and Mackman, R. L. (2017) Discovery and synthesis of a phosphoramidate prodrug of a pyrrolo[2,1-f][triazin-4-amino] adenine C-nucleoside (GS-5734) for the treatment of Ebola and emerging viruses. *J. Med. Chem.* 60, 1648–1661.